Sensitizing effect of Nd^{3+} on the Er^{3+}: 2.7 μm-emission in fluorophosphate glass

Lei Wen (温 磊)[1], Jianrong Wang (王建荣)[2], Lili Hu (胡丽丽)[1], and Liyan Zhang (张丽艳)[1*]

[1] *Key Laboratory of Materials for High Power Laser, Shanghai Institute of Optics and Fine Mechanics, Chinese Academy of Sciences, Shanghai 201800, China*

[2] *School of Materials Science and Engineering, Jinan University, Jinan 250022, China*

[*] *Corresponding author: jndxzly@hotmail.com*

Received July 2, 2011; accepted August 20, 2011; posted online October 18, 2011

Nd^{3+} strengthens the Er^{3+}:2.7-μm emission 10^4 times in fluorophosphate glass; in addition, it can also decrease its upconversion effects and the 1.5-μm emission accordingly. Cross-relaxation process is the principal transition mechanism in this codoping system. Compared with Er^{3+} singly doped glass, J-O parameters along with the A_{rad}, β, τ_R values of Er^{3+} change markedly in Er^{3+}:Nd^{3+} codoped glass because Nd^{3+} greatly influences the local environment around Er^{3+}. Results also show that Nd^{3+} has a good $^4I_{13/2}$ lifetime quenching effect as well as thermal load reduction ability for Er^{3+}:2.7-μm emission.

OCIS codes: 160.2290, 160.5690, 300.2140.

doi: 10.3788/COL201109.121601.

Mid-IR (MIR) lasers have significant applications in many areas, such as medicine, hazardous chemical detection, coherent lidar, remote atmospheric sensing, pollution monitoring, and MIR laser countermeasures weapon[1−5]. Er^{3+}:2.7-μm emission is a good MIR laser source, and has been utilized in many materials[3,6−10]. Because MIR emission is greatly influenced by the phonon energy of the gain media[11,12], materials with lower phonon energy are preferable in order to compensate for the large quantum defect of Er^{3+}:2.7-μm emission. Although the Er^{3+}:2.7-μm laser has been obtained in fluoride glass fiber, its thermal, chemical, and environmental properties, as well as its preparation properties, are not suitable for further applications. Fluorophosphate (FP) glass has been recognized as one of the most promising materials for MIR fiber lasers because of its better formation ability, crystallization stability, and fiber drawing properties compared with fluoride glass[13−15].

MIR emission in FP glass has rarely been reported. In this letter, we evaluate the effect of Nd^{3+} on Er^{3+}:2.7-μm emission in FP glass. Er^{3+}singly doped and Er^{3+}:Nd^{3+}codoped glass samples, labeled as Er and EN, were prepared according to the following compositions (in mol%): $3Al(PO_3)_3$-$5Sr(H_2PO_4)_2$-$52R_1F_2$-$40R_2F_3$ (R_1=Mg, Ca, Sr, Ba, R_2=Al, Y)-0.4ErF_3-(0,0.8)NdF_3. The glasses were prepared from reagent-grade fluorides, phosphates, and high-purity rare-earth fluorides by the conventional melting and quenching method. After annealing, the glasses were cut and polished to 20 × 10 × 3 (mm) for further measurements. Fluorescence spectra and lifetime, together with the upconversion luminescence, were recorded with a spectrofluorimeter (FLSP920, Edinburgh Instrument, VK) (measurement range of 200–3 300 nm) under the excitation of a 976-nm laser diode (LD). Moreover, absorption spectrum was measured by a UV/VIS/IR spectrophotometer (Lambda 900, Perkin Elmer, VSA) over a range of 300–2 000 nm.

As shown in Fig. 1, the 2.7-μm fluorescence is nearly unobservable in Er^{3+} singly doped glass; however, Nd^{3+}strengthens the fluorescence greatly. The inset shows the 1.5-μm fluorescence spectra, which is lower in EN than in Er. We also measured the $^4I_{13/2}$ lifetime, which were shown to be 10.8 and 2.4 ms in Er and EN, respectively. Apparently, the reduction of the 1.5-μm emission and the quenched $^4I_{13/2}$ lifetime in EN indicate that energy transfer process takes place on $^4I_{13/2}$ level, which can be depicted as (cross-relaxation) CR1: Er^{3+}:$^4I_{13/2}$+$^4I_{15/2}$ →Nd^{3+}:$^4I_{9/2}$+$^4I_{15/2}$ (see Fig. 2 for energy levels of Er^{3+} and Nd^{3+}). Thus, $^4I_{13/2}$ transfers its energy to Nd^{3+}, which activates the $^4I_{9/2}$ →$^4I_{15/2}$ transition while de-exciting itself to $^4I_{15/2}$ state. This provides a good explanation why the 1.5-μm fluorescence and lifetime decrease in EN. Because the particles on $^4I_{13/2}$ are reduced, the 2.7-μm:$^4I_{11/2}$ →$^4I_{13/2}$ transition is strengthened accordingly.

Figure 3 shows the upconversion luminescence of the samples. Except for the lower upconversion intensity of EN compared with Er, both perform similar upconversion characteristics, including the same peak wavelength. This indicates that they possess the same upconversion mechanisms. Based on the similar spectra shape, as well

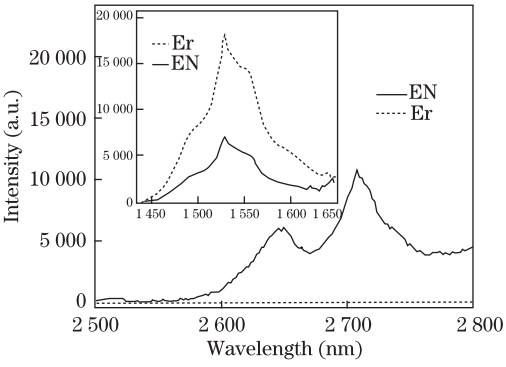

Fig. 1. Fluorescence spectra of Er and EN around 2.7 μm; inset shows the 1.5-μm emission.

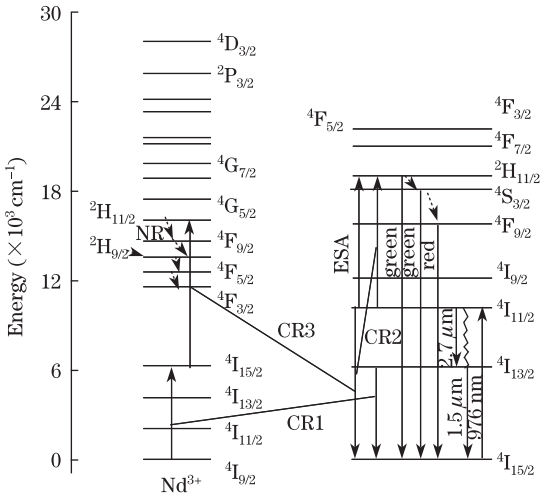

Fig. 2. Energy levels of $Nd^{3+}$and Er^{3+}.

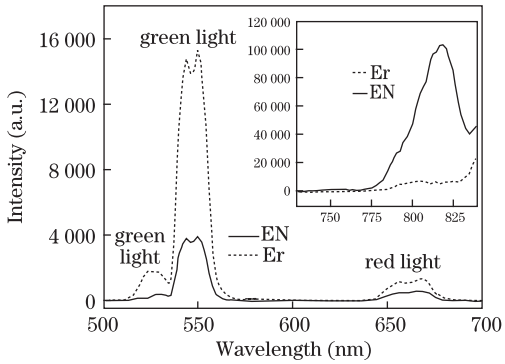

Fig. 3. Upconversion luminescences of Er and EN, inset is the fluorescence spectra around 804 nm.

as on the similar upconversion characteristics in Er and EN, the upconversion luminescence in EN is believed to be induced by Er^{3+}. The principal upconversion mechanisms of Er^{3+} are excited-state absorption (ESA) and cross-relaxations (CR2) processes; the uses of these mechanisms in various glasses have been discussed[14,16−18]. The CR1 process attenuates ESA and CR2 processes, resulting in decreased upconversion intensity in EN. Another possible energy transfer process involves particles on Er^{3+}:$^4I_{11/2}$ de-exciting to $^4I_{15/2}$, which activates the Nd^{3+}:$^4I_{15/2}$ $\rightarrow$$^2H_{11/2}$ transition through CR3 process. However, the four nonradiative (NR) relaxation processes from $^2H_{11/2}$ to $^4F_{3/2}$ consume energy; hence, no upconversion process occurs in Nd^{3+} ions. No other upconversion luminescence and 1.35/1.8-μm emissions from Nd^{3+}:$^4F_{3/2}$ were observed. Because the samples were measured under the 976-nm excitation, whether the Nd^{3+}: 0.93 and 1.06-μm emissions exist could not be determined.

To analyze the spectroscopic properties in Er and EN, J-O parameters ($\Omega_{2,4,6}$) further, spontaneous radiation probability $A_{\rm rad}$, branching ratio β together with the radiative lifetime $\tau_{\rm R}$ were calculated according to the J-O theory[19] (refer to Table 1). Figure 4 shows the absorption spectrum of Er and EN; the absorption bands of Er^{3+} are marked accordingly. First, J-O parameters significantly change in EN. Researcher know that $\Omega_{2,4,6}$ are closely related to the local characteristics around Er^{3+}. Because the base glass of Er and EN are completely the same, the greatly changed $\Omega_{2,4,6}$ values could only be attributed to the codoping with Nd^{3+}. This is because, with Nd^{3+} introduced, the local environment around Er^{3+} becomes changed markedly. The decreasing $\tau_{\rm R}$ value of EN coincides with the measured lifetime, and the increasing Ω_2 value means that the spontaneous radiation probability in EN would be higher than that in Er[20], which corresponds with the calculated results shown in Table 1. Clearly, the $A_{\rm rad}$ of $^4I_{11/2}$ $\rightarrow$$^4I_{13/2}$ transition is higher in EN, indicating that the 2.7-μm radiation tends to occur easily in EN. Interestingly, a radiative lifetime of $^4I_{9/2}$ is very high in EN, and has never been observed before. We then measured the corresponding fluorescence spectra of $^4I_{9/2}$(804 nm) in Er and EN glass. The inset of Fig. 3 shows that a much stronger fluorescence spectrum emerges at 804 nm in EN. This is believed to be induced by the Nd^{3+}:$^4F_{9/2}$,$^4F_{5/2}$ $\rightarrow$$^4I_{9/2}$ energy transfer process.

Table 1. $A_{\rm rad}$, β, $\tau_{\rm R}$, and $\Omega_{2,4,6}$ of Er and EN

Initial	End	Er			EN		
Level	Level	$A_{\rm rad}$(s^{-1})	β	$\tau_{\rm R}$(ms)	$A_{\rm rad}$(s^{-1})	β	$\tau_{\rm R}$(ms)
$^4I_{13/2}$	$^4I_{15/2}$	128.24	1	7.8	174.52	1	5.73
$^4I_{11/2}$	$^4I_{15/2}$	118.52	0.83	7.0	182.66	0.85	4.68
	$^4I_{13/2}$	24.35	0.17		31.23	0.15	
$^4I_{9/2}$	$^4I_{15/2}$	99.30	0.70	7.07	48.55	0.56	8.74
	$^4I_{13/2}$	40.79	0.29		64.00	0.43	
	$^4I_{11/2}$	1.86	0.01		1.86	0.01	
$^4F_{9/2}$	$^4I_{15/2}$	1 181.44	0.91	0.77	1 090.7	0.89	0.82
	$^4I_{13/2}$	57.32	0.05		48.18	0.04	
	$^4I_{11/2}$	54.24	0.04		83.57	0.07	
	$^4I_{9/2}$	1.34	0		1.58	0.00	
$^4S_{3/2}$	$^4I_{15/2}$	1 033.65	0.63	0.61	1 638.8	0.64	0.39
	$^4I_{13/2}$	523.03	0.32		829.28	0.32	
	$^4I_{11/2}$	32.10	0.02		49.1	0.02	
	$^4I_{9/2}$	48.95	0.03		63.9	0.03	
$\Omega_{2,4,6}$		2.77, 1.68, 1.47			3.27, 0.75, 2.33		
		$\delta = 0.17 \times 10^{-6}$			$\delta = 0.78 \times 10^{-6}$		

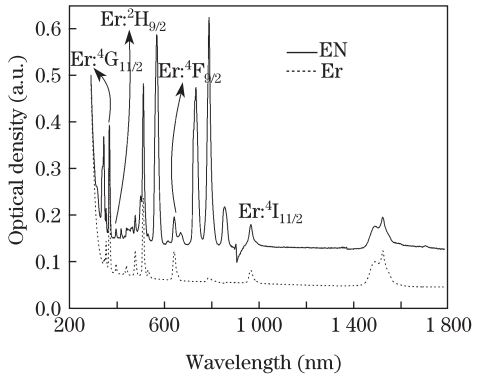

Fig. 4. Absorption spectra of Er and EN glasses. Absorption bands of Er^{3+} of EN are marked accordingly.

In conclusion, results show that Nd^{3+} not only strengthens Er^{3+}:2.7-μm emission greatly in FP glass, but also decreases its upconversion effects, which can significantly reduce thermal load of the glass. No other upconversions or emissions are observed in the glass. The cross-relaxation process is proven to be the principal transition mechanism in this codoping system. The J-O parameters, along with the $A_{\rm rad}$, β, $\tau_{\rm R}$ values of Er^{3+}, change significantly because the local environment around Er^{3+} is influenced greatly by the addition of Nd^{3+}.

This work was supported by the GF Innovation Fund of CAS under Grant No. CXJJ-11-S110.

References

1. M. Pollnau and S. D. Jackson, IEEE J. Sel. Top. Quantum Electron. **7,** 30 (2001).
2. T. Sanamyan, J. Simmons, and M. Dubinskii, in *OSA/CLEO/QELS 2010* CMDD6 (2010).
3. T. Sanamyan, J. Simmons, and M. Dubinskii, in *OSA/ASSP/LACSEA/LS&C2010* AMC3 (2010).
4. M. Zhong and G. Ren, www.cqvip.com.
5. C. Yu, D. He, G. Wang, J. Zhang, and L. Hu, Chin. Opt. Lett. **8,** 197 (2010).
6. M. Pollnau, R. Spring, S. Wittwer, W. Lüthy, and H. P. Weber, J. Opt. Soc. Am. B **14,** 974 (1997).
7. R. C. Stoneman and L. Esterowitz, Opt. Lett. **17,** 816 (1992).
8. B. J. Dinerman, P. F. Moulton, and D. M. Rines, Advanced Solid-State Lasers **15,** 396 (1993).
9. H. J. Eichler, B. Liu, J. Findeisen, A. A. Kaminskii, A. V. Butachin, and P. Peuser, Advanced Solid-State Lasers **10,** 222 (1997).
10. H. Yanagita, H. Toratani, T. Yamashita, and I. Masuda, Proc. SPIE **1513,** 387 (1991).
11. S. Dai, B. Peng, X. Wang, X. Shen, Q. Nie, and T. Xu, Acta Photon. Sin. (in Chinese) **37,** 239 (2008).
12. S. Feng, F. Luan, S. Li, L. Chen, B. Wang, W. Chen, L. Hu, Y. Guyot, and G. Boulon, Chin. Opt. Lett. **8,** 190 (2010).
13. L. Zhang, H. Sun, S. Xu, K. Li, and L. Hu, J. Lumin. **117,** 46 (2006).
14. L. Zhang, H. Sun, S. Xu, K. Li, and L. Hu, Solid State Commun. **135,** 449 (2005).
15. M. Wang, L. Yi, G. Wang, L. Hu, and J. Zhang, Solid State Commun. **149,** 1216 (2009).
16. H. U. Güdel and M. Pollnau, J. Alloys. Compd. **303-304,** 307 (2000).
17. F. Auzel, J. Lumin. **72-74,** 152 (1997).
18. A. S. Oliveira, M. T. de Araujo, A. S. Gouveia-Neto, A. S. B. Sombra, J. A. Medeiros Neto, and N. Aranha, J. Appl. Phys. **83,** 604 (1998).
19. W. T. Carnall, P. R. Fields, and K. Rajnak, J. Chem. Phys. **49,** 4412 (1968).
20. T. Murata, K. Mazeno, and K. Morinaga, Sci. Tech. Adv. Mat. **3,** 85 (2002).